GEOPHYSICAL RESEARCH LETTERS, VOL. 22, NO. 13, PAGES 1661-1664, JULY 1, 1995

The great Kurile earthquake of October 4, 1994 tore the slab

Yuichiro Tanioka, Larry Ruff, and Kenji Satake

Dept. of Geological Science, University of Michigan, Ann Arbor

Abstract. The fault geometry, depth, and slip distribution of the Kurile earthquake of Oct. 4, 1994 are estimated using seismic waveforms, aftershock distribution, geodetic measurements, and tsunami waveforms. Previous large earthquakes in the Kurile arc had typical underthrusting focal mechanisms due to the local subduction. Seismic wave inversions of the 1994 event indicate a thrust type mechanism with a large strike-slip component. This does not represent an underthrust event at the subduction interface. The focal depth is estimated at 50 km, just beneath the previously estimated subduction interface. We calculate crustal deformation and tsunami waveforms from the two possible fault planes of the focal mechanism solution and find that both fault planes explain the observations. We choose the north-south striking plane, because of the occurrence of a large (M_W 7.8) intermediate-depth earthquake on Dec. 6, 1978, northwest of the 1994 rupture area. The lineation of aftershock distributions of these two events suggests that both earthquakes were due to a tearing of the slab perpendicular to the trench. The joint inversion of geodetic and tsunami data shows that the largest slip, about 17 m, occurred at the upper end of the slab.

Introduction

A great earthquake occurred off Shikotan Island along the Kurile trench on October 4, 1994. The NEIS Preliminary Determination of Epicenters (PDE) provides the source parameters: origin time, 13:22:59.54 GMT; epicenter, 43.956°N, 147.412°E; magnitude, M_S 8.1. The seismic moment from the Harvard Centroid Moment Tensor (CMT) solution is 35×10^{20} Nm (M_W 8.3). This earthquake and tsunami caused great damage to Shikotan Island. This was the largest earthquake shallower than 100 km since the Macquarie Ridge earthquake of May 23, 1989 (M_S=8.2).

Many large earthquakes have occurred due to the subduction along the Kurile trench. Figure 1 shows the most recent sequence of great underthrusting events to rupture the Kurile subduction zone. The entire southern part of the Kurile arc ruptured in a series of large earthquakes that started with the 1952 event off Hokkaido, continued with the 1958 and 1963 events at the northern part, the 1968 event at the southern end, the 1969 event just to the south of the 1958 event, and then finished with the 1973 event between the 1952 and 1969 events. *Fukao and Furumoto* [1979] *and Schwartz and Ruff* [1987] studied the rupture process of some of these events and found the dominant asperities for each large earthquake. The maximum coseismic slip of the asperities is about 7 m for the single large asperity that ruptured in the 1969 event. Thus, assuming that the convergence rate is about 9 cm/yr in this region, the tectonic motions need to accumulate for 78 years to equal the slip in the asperity of the 1969 earthquake. The seismic potential map of *McCann et al.* [1979] assigned the entire Kurile arc to the category of lowest potential for great earthquakes. The most recent update of *Nishenko* [1991] assigned the 1969 rupture area a probability of less than 20% to have a great plate boundary earthquake in the ten-year period 1989-1999.

In this paper, we use all available observations: seismic waveforms, aftershock distribution, geodetic measurements, and tsunami waveforms, to determine the source process of the Oct. 4, 1994 great earthquake and to answer the key question: was the 1994 earthquake a rerupture of the 1969 underthrusting plate boundary event? If not, what is the tectonic characteristics of this earthquake?

Paper number 95GL01656
0094-8534/95/95GL-01656$03.00

Method and Data

Seismological Analysis

The Moment Tensor Rate Function (MTRF) inversion [*Ruff and Miller*, 1994] was performed using the 16 P and 3 SH waves recorded at IRIS stations to estimate the best depth and focal mechanism of the earthquake (Figure 2). The Centroid Moment Tensor (CMT) inversion [*Dziewonski et al.*, 1981] was performed using 19 IRIS stations (ADK, AFI, ANMO, BOSA, CCM, COL, CTAO, DPC, FFC, GUMO, HRV, KEV, KIP, LAPZ, PAB, PAS, SJG, TAU, and TBT) to estimate the overall focal mechanism of the earthquake. We compare these estimates with those from Harvard CMT, Earthquake Research Institute (ERI) CMT, U.S. Geological Survey (USGS) moment tensor inversions and an analysis by *Kikuchi and Kanamori* [1995].

Geodetic Analysis

Coseismic displacement provides constraints on the fault geometry and slip on the fault. The Geographical Survey Institute of Japan recently installed a network of continuous recording GPS stations which detected horizontal coseismic displacements at 5 stations in Hokkaido [*Tsuji et al.*, 1995]. These results were available within a few days after the Oct. 4, 1994 earthquake. Subsidence of 53 cm of Shikotan Island, which is the closest island to the epicenter, was also observed [*Yeh et al.*, 1995]. The vertical and horizontal displacement are computed using *Okada*'s [1985] formulas and compared with the observations.

Tsunami Analysis

Tsunami waveforms also provide constraints on the actual fault geometry and slip on the fault. The tsunami waveforms at 13 tide gauge stations, 7 in Hokkaido, 5 in Honshu, and 1 on Shikotan Island, are compared with the computed tsunamis. The tsunami waveforms are numerically computed using the actual bathymetry. The method of computation is the same as *Satake* [1989]. The finite difference computation of the linear long wave equation and the equation of continuity is carried out with a grid size of 1 minute (less than 2 km).

Joint Inversion of Geodetic and Tsunami Data

Slip distribution of the 1994 Kurile earthquake is determined by a joint inversion of tsunami and geodetic data. We used the 13

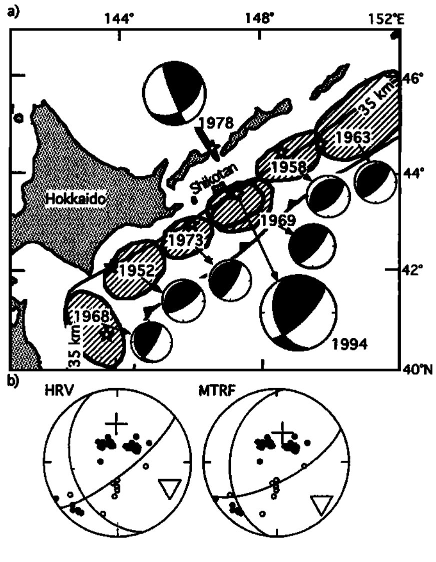

Figure 1. (a) The source regions and focal mechanisms of the last sequence of great earthquakes to rupture the Kurile arc [*Fukao and Furumoto,* 1979], the Dec. 6 1978 Kunashiri strait and Oct. 4 1994 Kurile earthquakes. The focal mechanism for the 1994 event is the result from our CMT analysis. The stars show the epicenters. The 35 km depth contour of the plate interface [*Tichelaar and Ruff,* 1993] is also shown. (b) Two focal mechanisms of the 1994 Kurile earthquake with the P-wave first motions (open, dilatational; closed, compressional), the Harvard CMT (HRV) and Moment Tensor Rate Function (MTRF) inversions. Crosses are the T-axis and triangles are the P-axis.

tsunami waveforms and the 5 horizontal displacements, which have been described above. The tsunami waveforms for each tide gauge station consist of 25 -100 min of data point with a sampling interval of 1 min. The method of joint inversion of tsunami and geodetic data is described in *Satake* [1993]. For error analysis, we applied the jackknifing technique [e.g. *Tichelaar and Ruff,* 1989].

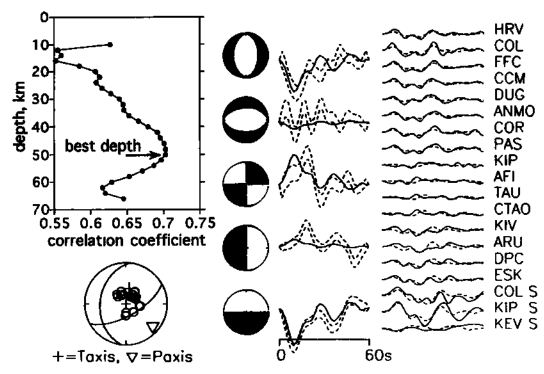

Figure 2. (top left) The correlation coefficient between the observed and synthetic waves as a function of depth. (bottom left) The best double couple focal mechanism. (center) The Moment Tensor Rate Functions (MTRFs); dashed traces are the uncertainty range and solid traces are the source time function re-scaled for the double couple solution. (right) The observed (solid) and synthetic (dashed) seismograms for the listed stations in azimuthal order. S after the station name indicates SH-wave.

Focal Mechanism

A plate interface earthquake in the 1994 rupture area would be characterized by a fault geometry of "thrusting" on a fault plane that dips to the northwest at a shallow angle. The focal mechanism solution of the 1994 event from our CMT is shown in Figure 1a. The focal mechanisms from Harvard CMT and MTRF inversion with the available P wave first motions are shown in Figure 1b. Both the CMT and MTRF focal mechanisms explain most first motions around the world. Additional determination of focal mechanism by Earthquake Research Institute in Japan, USGS and *Kikuchi and Kanamori* [1995] give the same basic geometry as shown in Figure 1. The focal mechanisms of the 1994 Kurile event from five different determinations indicate a thrust-type faulting with a large strike-slip component, which does not represent a plate interface event. The consistency between these five estimates over a wide frequency range and the P wave first motions suggests that this focal mechanism represents the entire rupture process.

Depth

The best depth from the MTRF inversion is 50 km (Figure 2). The USGS moment tensor best depth is 45 km. The best depth from *Kikuchi and Kanamori* [1995] is 50 km. The centroid depth from the Harvard and ERI CMT is 59 and 42 km, respectively. Thus, there appears to be a fairly good agreement that the best overall depth estimate lies between 42 and 59 km. In a recent global survey, *Tichelaar and Ruff* [1993] mapped the deepest extent of the seismogenic plate interface in subduction zones. They found that the underthrusting events in the Kurile arc occur at a depth of 40 km or less. If the entire width of the plate interface ruptures with the same slip amount, then the average depth for such an earthquake would be around 20 km, not 50 km. The best depth of the 1994 Kurile event is just below the seismogenic interface, suggesting that it is not a plate interface event, rather it is an intraplate event within the subducting lithosphere.

Fault Geometry

Figure 3 shows the observed horizontal coseismic displacements at the 5 GPS stations in the eastern Hokkaido,

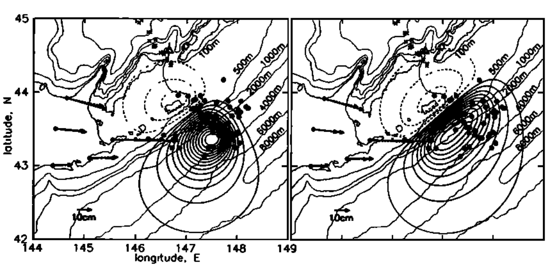

Figure 3. Geodetic deformation is calculated for two fault models: (left) a north-south fault; and (right) a northeast-southwest fault, based on the CMT focal mechanism. Maps show mainshock (solid triangle) and aftershocks (solid circles) of the 1994 Kurile event, mainshock (open triangle) and aftershocks (crosses) of the 1978 event, and bathymetry. Observed and computed coseismic horizontal displacements are shown as solid and dashed arrows, respectively. Coseismic horizontal displacements are observed by Geographical Survey Institute in Japan [*Tsuji et al.,* 1994]. Closed contours show calculated vertical deformation (solid curves for uplift and dashed for subsidence with a 20 cm interval).

referenced to Usuda in central Japan [*Tsuji et al.*, 1995]. The figure also shows the calculated vertical and horizontal displacements from two fault models derived from the nodal planes of the focal mechanism. One fault strikes approximately north-south (strike 160°, dip 40°, rake 30°). The length and width of the fault are assumed to be 60 km and 70 km, respectively. The average slip on the fault is calculated as 13.9 m from the seismic moment 35×10^{20} Nm assuming that the rigidity is 6×10^{10} N/m^2. The other fault model strikes northeast-southwest, parallel to trench (strike 50°, dip 70°, rake 125°). The length and width of the fault plane are 120 km and 45 km, respectively. The average slip on this fault is calculated as 10.8 m. The figure shows that either fault model can match both the direction and approximate magnitude of the coseismic displacements. Computed tsunami waveforms from the two fault models also indicate that either fault model can equally explain the observed tsunami waveforms.

Important information for the identification of the fault geometry is provided from a large earthquake (Mw=7.8) that occurred on Dec. 6, 1978, at a depth of about 100 km, northwest of the 1994 epicenter (Figure 1). The 1978 event has been interpreted as a tearing motion within the subducting slab [*Kasahara and Sasatani*, 1985;*Lundgren et al.*, 1988]. *Moriya* [1990] also suggests the possibility of the slab tearing near the 1978 event from seismicity analysis. Figure 3 shows aftershocks (crosses) of the 1978 event from *Kasahara and Sasatani* [1985] and one day aftershocks (solid circles) of the 1994 event from the PDE. The lineation of the 1978 aftershocks and many of the 1994 aftershocks are clearly seen, although the aftershock distribution determined from local seismic stations in Hokkaido, Japan [*Katsumata et al., 1995*] does not show such a clear lineation. This lineation is perpendicular to the trench axis. We suggest that the 1994 event is the trenchward continuation of the 1978 event which tore the subducting slab with a left-lateral strike slip motion in the slab (Figure 4). This indicates that the north-south trending nodal plane is the fault plane of the 1994 event. However, the strike of the lineation of the 1994 aftershocks is about 20°-30° to the west from the strike of the fault plane. This difference, denoted as θ in Figure 4, is explained by the shallow dip angle of the fault plane, about 40°, and the shallow dip angle of the subducting slab, about 20°, if we assume that the aftershocks are concentrated in the uppermost part of the slab which represents the top of the rupture zone ($\theta = \arcsin(\tan20° / \tan40°) = 26°$). This assumption is reasonable because the top of the slab is the most brittle part.

Using the Harvard CMT catalog, we also analyzed 21 aftershocks that occurred within one month of the Oct. 4 event.

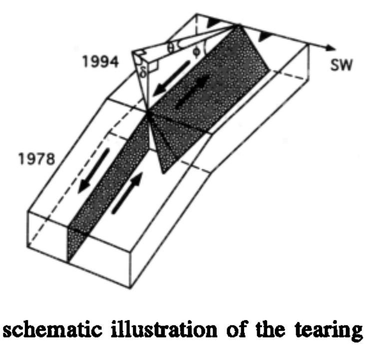

Figure 4. A schematic illustration of the tearing motion of the subducting slab by the 1978 Kunashiri strait and 1994 Kurile events. Dip angle of slab is ϕ, dip angle of the fault plane is δ, and the angle between the fault strike and the projection of top of the rupture area is θ.

Six of the 21 aftershocks were located on the northeast side of the lineation; the other 15 were located on the southwest side or directly on the lineation (Figure 5). The aftershocks on the northeast side include 4 underthrust-type events (open circles in Figure 5), but no event with a mainshock-type focal mechanism. On the other hand, the aftershocks on the southwest side include 7 mainshock-type events (solid circles in Figure 5) and 3 underthrust-type events. This suggests that the rupture area of the mainshock is actually on the southwest side of the lineation and the mainshock triggered the faulting on the plate interface on the northeast side. One previous example of similar aftershock sequences is the 1977 Tonga events [*Christensen and Lay*, 1988].

Slip Distribution

We use the north-south trending fault plane (strike 160°, dip 40°, rake 30°) for the joint inversion of tsunami and geodetic data. The fault area is divided into four subfaults as shown in Figure 5. The top edge of the fault plane is on the top surface of the subducting plate which is dipping 20° to the north-west. The depths for the shallowest corner of each subfault are 23.7 km for subfault A, 12.5 km for B, 46.2 km for C, and 35.0 km for D. The length and width of all subfaults are 45 km and 35 km, respectively. The result of the joint inversion is also shown in Figure 5. The observed and synthetic tsunami waveforms show a good agreement (Figure 6). The computed horizontal displacements also agree with the observations. The observed subsidence of Shikotan Island, 53 cm, is well reproduced although this information was not used for the inversion. The largest slip, 16.8 m, was on subfault A, which is located in the upper side of the rupture zone. The depth range of subfault A is 23.7 - 57.5 km, which includes the best depth of 50 km

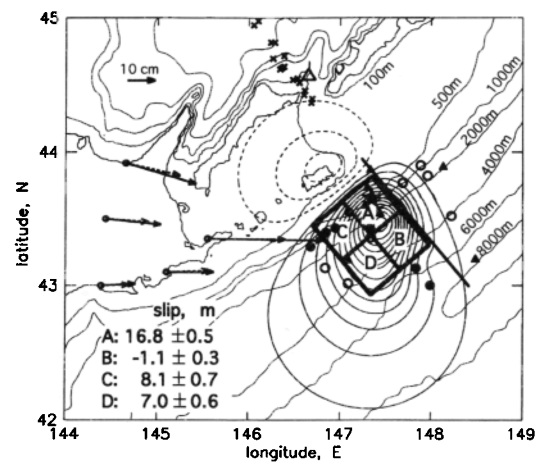

Figure 5. The result of the joint inversion. Open triangle and crosses are mainshock and aftershocks of the 1978 event, respectively. Open circles (underthrust-type), closed circles (mainshock-type mechanism), closed triangles (other mechanism) are one month aftershocks from the Harvard CMT catalog. The solid line shows the northeast edge of the lineation of one day aftershocks of the 1994 event. Solid and dashed arrows are the observed and computed horizontal displacements, respectively. Closed contours show vertical displacement (solid curves for uplift and dashed for subsidence with a 20 cm interval). Frames show the location of four subfaults. The numbers at the left bottom corner show the slip distribution on each subfault.

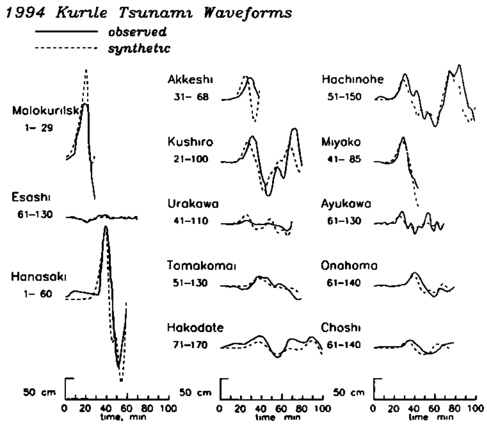

Figure 6. Comparison of the observed (solid) and computed (dashed) tsunami waveforms from the joint inversion. The numbers below the station name indicate the time period of the waveforms (in min after the origin time of the event.)

determined from the seismological analysis. The second and third largest slips, 8.1 m and 7.0 m, were estimated on subfaults C and D, respectively, which are located at the lower side of the rupture zone. This indicates that the largest moment was released in the upper half of the fault. The total seismic moment from subfaults A, C, and D is 30×10^{20} Nm by assuming that the rigidity is 6×10^{10} N/m^2. This is consistent with our CMT estimate, 27×10^{20} Nm , and the Harvard CMT estimate, 35×10^{20} Nm, but slightly larger than the MTRF estimate, 13×10^{20} Nm, and the ERI CMT estimate, 13×10^{20} Nm. *Kikuchi and Kanamori* [1995] suggested that the scatter of the seismic moment estimates is partly due to the large vertical extent of the source. Our joint inversion indicates that the smaller moment release occurred on deeper subfaults C and D.

Discussion and Conclusion

We conclude that the Oct. 4, 1994 great Kurile earthquake was not a rerupture of the 1969 underthrusting event, rather it was an intra-slab event. Most of the well-known great intra-slab events occur in the outer-rise [*Christensen and Ruff,* 1988] (examples are the 1933 Sanriku, and 1977 Sumba, Indonesia events), and they have been interpreted as a consequence of slab pull being transmitted to the trench axis. There are a few other examples of normal faulting at intermediate depths, just at the down-dip side of the underthrusting interface, such as the 1977 Tonga event [*Christensen and Lay,* 1988]. The 1994 Kurile event does not exactly correspond to any of these well-known examples. It was a tearing event of the subducting oceanic lithosphere along a direction perpendicular to the trench. Is the 1994 Kurile event a unique event? Or, have many large events like this occurred in the past, but been mistaken for underthrusting earthquakes? This important question awaits future studies.

One consequence of our conclusion is that the 1994 Kurile event does not violate the seismic gap hypothesis, nor the seismic potential map of *Nishenko* [1991] as strictly interpreted, because the event was not an interplate event. On the other hand, a great earthquake is quite hazardous, whether it occurs at a plate boundary or not. For the purpose of seismic hazard analysis, it is important to include such intraplate earthquakes.

Acknowledgments. We thank J. Johnson for helpful comments. The tide gauge records in Japan were provided by Dr. Y. Tsuji at Earthquake Research Institute, University of Tokyo. The tide gauge record at Malokurilsk was provided by H. Yeh in University of Washington. GPS data were provided by H. Tsuji at the Geographical Survey Institute in Japan. This work was supported by National Science Foundation (EAR 9405767 and EAR 9405533).

References

Christensen, D.H. and T. Lay, Large earthquakes in the Tonga region associated with subduction of the Louisville ridge. *J. Geophys. Res., 93,* 13367-13389, 1988.

Christensen, D.H. and L.J. Ruff, Seismic coupling and outer rise earthquakes, *J. Geophys. Res., 93,* 13421-13444, 1988.

Dziewonski, A.M., T.A. Chou, and J.H. Woodhouse, Determination of earthquake source parameters from waveform data for studies of global and regional seismicity, *J. Geophys. Res., 86,* 2825-2853, 1981.

Fukao, Y. and M. Furumoto, Stress drops, wave spectra and recurrence intervals of great earthquakes - Implications of the Etorofu earthquake of 1958 November 6, *Geophys. J. R. astr. Soc.,* 57, 23-40, 1979.

Kasahara, M., and T. Sasatani, Source characteristics of the Kunashiri strait earthquake of December 6, 1978 as deduced from strain seismograms, *Phys. Earth Planet. Inter., 37,* 124-134, 1985.

Katsumata, K., M. Ichiyanagi, M. Miwa, H. Miyamachi, and M. Kasahara, Aftershock distribution of the October 4, 1994 Mw8.3 Kurile islands earthquake by a local seismic network in Hokkaido, Japan, *Geophys. Res. Lett.,* in press, 1995.

Kikuchi, M., and Kanamori, H., The Shikotan earthquake of October 4, 1994: A lithospheric earthquake, *Geophys. Res. Lett., 22,* 1025-1028, 1995.

Lundgren, P.R., E.A. Okal, and S. Stein, Body-wave deconvolution for variable source parameters; application to the 1978 December 6 Kurils earthquake, *Geophys. J., 94,* 171-180, 1988.

McCann, W.R., S.P. Nishenko, L.R. Sykes, and J. Krause, Seismic gaps and plate tectonics: seismic potential for major boundaries, *Pure Appl. Geophys., 117,* 1082-1147, 1979.

Moriya, T., Is the Kurile slab torn beneath Kunashiri strait? *Abstracts of the 1990 fall meeting of the Seismological Society of Japan, 2,* 162, 1990 (in Japanese).

Nishenko, S.P., Circum-Pacific seismic potential, 1989-1999, *Pure Appl. Geophys., 135,* 169-259, 1991.

Okada, Y., Surface deformation due to shear and tensile faults in a half-space, *Bull. Seism. Soc. Am., 75,* 1135-1154, 1985.

Ruff, L.J., and A.D. Miller, Rupture process of large earthquakes in the northern Mexico subduction zone, *Pure Appl. Geophys., 142,* 101-172, 1994.

Satake, K., Inversion of tsunami waveforms for the estimation of heterogeneous fault motion of large submarine earthquakes: the 1968 Tokachi-oki and the 1983 Japan Sea earthquakes, *J. Geophys. Res., 94,* 5627-5636, 1989.

Satake, K., Depth distribution of coseismic slip along the Nankai Trough, Japan, from joint inversion of Geodetic and tsunami data, *J. Geophys. Res., 98,* 4553-4565, 1993.

Schwartz, S.Y., and L.J. Ruff, Asperity distribution and earthquake occurrence in the southern Kuril Islands Arc, *Phys. Earth Planet. Inter., 49,* 54-77, 1987.

Tichelaar, B.W., and L.J. Ruff, How good are our best models? Jackknifing, bootstrapping, and earthquake depth, *Eos, 70,* 593, 605-606, 1989.

Tichelaar, B.W., and L.J. Ruff, Depth of seismic coupling along subduction zones, *J. Geophys. Res., 98,* 2017-2037, 1993.

Tsuji, H., Y. Hatanaka, T. Sagiya, and M. Hashimoto, Coseismic crustal deformation from the 1994 Hokkaido-Toho-Oki earthquake monitored by a nationwide continuous GPS array in Japan, *Geophys. Res. Lett.,* in press, 1995.

Yeh, H., V. Titov, V. Gusiakov, E. Pelinovsky, V. Khramushin, and V. Kastrenko, The 1994 Shikotan earthquake tsunamis, *Pure Appl. Geophys.,* in press, 1995.

L.J. Ruff, K. Satake and Y. Tanioka, Dept. of Geological Sciences, Univ. of Michigan, Ann Arbor, MI 48109-1063. (e-mail: ruff@umich.edu, kenji@umich.edu, tanioka@umich.edu)

(Received March 9, 1995; revised May 8, 1995; accepted May 8, 1995.)